Published in final edited form as:
Int J Cancer. 2010 March 15; 126(6): 1403–1416. doi:10.1002/ijc.24938.

The Arf-inducing Transcription Factor Dmp1 Encodes a Transcriptional Activator of Amphiregulin, Thrombospondin-1, JunB and Egr1

Ali Mallakin[1,2,†], **Takayuki Sugiyama**[1,2,†], **Fumitake Kai**[1,2,†], **Pankaj Taneja**[1,2], **Robert D. Kendig**[1,2], **Donna P. Frazier**[1,2], **Dejan Maglic**[1,2,3], **Lauren A. Matise**[1,2], **Mark C. Willingham**[1], and **Kazushi Inoue**[1,2,3,*]

[1] Department of Pathology, Wake Forest University Health Sciences, Medical Center Boulevard, Winston-Salem, NC 27157, USA

[2] Department of Cancer Biology, Wake Forest University Health Sciences, Medical Center Boulevard, Winston-Salem, NC 27157, USA

[3] Graduate Program in Molecular Medicine, Wake Forest University Health Sciences, Medical Center Boulevard, Winston-Salem, NC 27157, USA

Abstract

Dmp1 (Dmtf1) encodes a Myb-like transcription factor implicated in tumor suppression through direct activation of the Arf-p53 pathway. The human *DMP1* gene is frequently deleted in non-small cell lung cancers, especially those that retain wild-type *INK4a/ARF* and/or *p53*. To identify novel genes that are regulated by Dmp1, transcriptional profiles of lung tissue from *Dmp1*-null and wild-type mice were generated using the GeneChip Microarray. Comparative analysis of gene expression changes between the two groups resulted in identification of numerous genes that may be regulated by *Dmp1*. Notably, amphiregulin (*Areg*), thrombospondin-1 (*Tsp-1*), *JunB*, *Egr1*, adrenomedullin (*Adm*), *Bcl-3* and methyl-CpG binding domain protein 1 (*Mbd1*) were downregulated in the lungs from *Dmp1*-null mice while *Gas1* and *Ect2* genes were upregulated. These target genes were chosen for further analyses since they are involved in cell proliferation, transcription, angiogenesis/metastasis, apoptosis, or DNA methylation, and thus could account for the tumor suppressor phenotype of Dmp1. Dmp1 directly bound to the genomic loci of *Areg*, *Tsp-1*, *JunB* and *Egr1*. Significant upregulation or downregulation of the novel Dmp1 target genes was observed upon transient expression of Dmp1 in alveolar epithelial cells, an effect which was nullified by the inhibition of *de novo* mRNA synthesis. Interestingly, these genes and their protein products were significantly downregulated or upregulated in the lungs from *Dmp1*-heterozygous mice as well. Identification of novel Dmp1 target genes not only provides insights into the effects of Dmp1 on global gene expression, but also sheds light on the mechanism of haploid insufficiency of *Dmp1* in tumor suppression.

Keywords

Dmp1; Dmtf1; GeneChip Microarray; Lung; Amphiregulin; Thrombospondin-1; JunB; Egr1; Ect2; Arf; haploid insufficiency

[*]Corresponding author: 2102 Gray Building, Department of Pathology, Wake Forest University Health Sciences, Medical Center Boulevard, Winston-Salem, NC 27157, USA, kinoue@wfubmc.edu; Phone: +1 336 716 5863; FAX: +1 336 716 6757.
[†]These authors contributed equally to this work.

Introduction

Dmp1 (cyclin D binding myb-like protein 1; also called Dmtf1) is a transcription factor that was originally isolated in a yeast two-hybrid screen of a murine T-lymphocyte library with cyclin D2 as bait.[1–3] Dmp1 binds to the DNA consensus sequences CCCG(G/T)ATG(T/C), a subset of which are also bound by proteins of the Ets family.[4–6] Generally, Ets proteins are known to act as positive or negative regulators of genes expressed in various biological processes, including those that control cellular proliferation, differentiation, apoptosis, metastasis, tissue remodeling, angiogenesis and transformation.[7] It follows that Dmp1 may potentially play roles in these biological processes as well. Dmp1 mRNA is ubiquitously expressed in normal mouse tissue; its protein levels are highest in the testis and thymus, followed by the lungs and brain.[8, 9]

We have accumulating evidence for transcriptional regulation of Dmp1. The *Dmp1* promoter receives oncogenic signals from activated Ras via the Raf-MEK-ERK-Jun pathway which, in turn, causes activation of the $p19^{Arf}$ promoter and induces cell cycle arrest to quench oncogenic signaling.[10] Conversely, the *Dmp1* promoter is repressed by physiological mitogenic stimuli and overexpression of E2F proteins.[9] The *Dmp1* promoter is also repressed by genotoxic stimuli mediated by NF-κB[11] and by the Wilms tumor gene product, WT1.[12] Both *Dmp1*-knockout and heterozygous mice are prone to tumor development. Tumors isolated from $Dmp1^{+/-}$ mice seldom lose the wild-type *Dmp1* allele, indicating that *Dmp1* is haplo-insufficient for tumor suppression.[13–14] Deletion or mutation of *Arf* or *p53* is rare in tumors from *Dmp1*-knockout mice. Thus, *Dmp1* has been considered a physiological regulator of the Arf-p53 pathway *in vivo*.[2,3,13,14]

When Dmp1 expression was studied *in vivo* using specific antibodies, the protein was expressed in alveolar macrophages and type II cells in the lung.[9] The *Dmp1* gene was deleted in 40 % of $K\text{-}ras^{LA}$ lung cancers, and the gene deletion was mutually exclusive with mutations of the *p53* gene.[14] Likewise, loss of heterozygosity (LOH) of the human *DMP1* gene (h*DMP1*) is found in ~35 % of human non-small-cell lung carcinomas (NSCLC), suggesting the primary involvement of h*DMP1* in lung carcinogenesis.[14] The LOH of h*DMP1* was found in a mutually exclusive fashion with those of $p14^{ARF}$ and/or *p53* in 80–90 % of the cases, indicating that *h*DMP1 is a physiological regulator of the ARF-p53 pathway in human tissues as well.[2,3,14]

In this study, high-density oligonucleotide microarrays were utilized to identify previously unknown target genes for the *Dmp1* transcription factor that are involved in tumor suppression, tumorigenesis, and cell cycle regulation.[15–18] Real-time reverse transcription PCR (RT-PCR) of selected genes validated the microarray results and demonstrated a wide range of differentially expressed genes. Here we report that several genes that are involved in cell cycle/proliferation/transcription (*amphiregulin*, *adrenomedullin*, *JunB* and *Egr1*), angiogenesis and metastasis (*thrombospondin-1*), apoptosis (*Bcl-3*), and DNA methylation (*methyl DNA-binding protein 1*) were found to be downregulated in tissues of *Dmp1*-deficient mice, and thus, they could represent novel transcriptional targets for Dmp1. We also identified genes that were upregulated in the lungs (*Gas1* and *Ect2*, cell cycle/proliferation) from $Dmp1^{-/-}$ mice. The genes identified in this study constitute promising candidates for further studies to clarify the unrevealed functions and novel signaling pathways regulated by Dmp1.

Materials and Methods

Dmp1-knockout mice

The mice used in this experiment contained a targeted disruption of *Dmp1* as described previously.8 Two $Dmp1^{+/-}$ females were backcrossed with a single C57BL/6 male for more than 8 generations to minimize the effects of strain-dependent difference of gene expression. The mice were overall >99 % pure for C57BL/6 at G8. All 7 markers on mouse chromosome 5 where *Dmp1* is located had been replaced with C57BL/6 markers at G8. Mice were observed daily and maintained in accordance with the Guide for the Care and Use of Laboratory Animals.

Gene expression profiling with Affymetrix 430A microarrays

For each phenotype, RNA was pooled from three separate mice (4 to 6 weeks of age) of the same genotype. Total RNA was isolated from the homogenized lung tissues of *Dmp1* wild-type and knock-out mice utilizing Trizol reagent (Invitrogen, Carlsbad, CA) according to the manufacturer's instructions. RNA pellets were resuspended in nuclease-free water (Sigma, St. Louis, MO). The quality of RNA was determined spectrophotometrically using an Agilent 2100 Bioanalyzer. First-strand cDNA synthesis was accomplished utilizing the Oligo dT primer method and Superscript II enzyme provided by a One-Cycle-cDNA Affymetrix Synthesis Kit # 900431 (Affymetrix, Santa Clara, CA). From cDNA, cRNA was synthesized using the Affymetrix IVT labeling kit # 900449. Synthesized cRNA was labeled during transcription (MEGAscript® system; Ambion, Inc., Austin, TX) with biotin-11-cytidine triphosphate and biotin-16-uridine triphosphate (Enzo Diagnostics, Farmingdale, NY).

Biotinylated cRNA products were hybridized to Affymetrix GeneChip arrays (murine GeneChip 430A) for 16 hours at 45°C using the manufacturer's hybridization buffer. After hybridization, GeneChip arrays were washed and stained by a fluidics station 450 using the ProkGE-WS2 fluidics script (Affymetrix). Once the probe arrays were hybridized and washed, they were scanned using the Affymetrix GeneChip 7G plus scanner (Hewlett-Packard Gene array scanner G2500A; Affymetrix) according to the manufacturer's procedures. The known Dmp1 target gene, *Cdkn2a* ($p19^{Arf}$/$p16^{Ink4a}$, exons 2–3) was expressed at very low levels in wild-type lungs, but was not detectably expressed in $Dmp1^{-/-}$ lungs by our murine GeneChip 430A array, confirming the reliability of our GeneChip microarray.

Data Analysis

To process the primary quantitative data from each hybridizationexperiment, probe signals in raw CEL files were summarized using MicroArray Suite 4.0 (Affymetrix) and the expression data was then analyzed by Genesis software (Institute for Genomics and Bioinformatics - Graz University of Technology, Graz, Austria). To determine if the RNA abundance corresponding to each gene encoded on the array was detectable, several factors were evaluated, including the number of parameters representing each gene in which the intensity of the perfect match hybridization reaction exceeded that of the mismatch hybridization signal and the perfect match/mismatch ratios for each set of corresponding probe pairs. The raw data were then normalized on a per-chip basis for both $Dmp1^{+/+}$ and $Dmp1^{-/-}$ lung samples. In this way, one is able to see differences between $Dmp1^{+/+}$ and $Dmp1^{-/-}$ animals. Gene induction was considered significant if the change in this normalized intensity was above 2-fold.

Identification of gene expression patterns

To identify the genes that were differentially expressed in lung tissues of wild-type and *Dmp1*-null mice, Genesis software was utilized. A total of 300 probe sets, corresponding to 250 unique genes and few expressed sequence tags, were identified based onany expression that differed by 2-fold or more between $Dmp1^{+/+}$ and $Dmp1^{-/-}$ tissue samples. The differentially expressed transcripts were clustered according to their expressionprofiles utilizing a K-means algorithm in the Genesis software. K-means analysis places gene expression profiles into a predefinednumber of clusters based on relative expression across the sample series.

Real-time PCR

To validate the gene expression levels determined by microarray analysis, the expression of several candidate genes including *Areg*, *Tsp-1*, *JunB*, *Egr1*, *Bcl-3*, *Adm*, *Mbd1*, *Gas1* and *Ect2* were checked by real-time quantitative PCR with an ABI 7500 system.9,14 Taqman assays specific to cDNAs were used in the study (Applied Biosystems [ABI], Foster City, CA). The ID number of TaqMan primers and probes obtained from ABI were as follows: *Areg*: Mm00437583_m1, *Tsp-1*: Mm00449022_m1, *Jun*B: Mm00492781_s1, *Egr1*: Mm00656724_m1; *Bcl-3*: Mm00504306_m1, *Adm*: Mm00437438_g1, *Mbd1*: Mm00522100_m1, *Gas1*: Mm01700206_g1, *Ect2*: Mm00432964_m1, $p27^{kip1}$: Mm00438168_m1, and internal control *β-actin*: Mm02619580_g1. Specific primers for *Dmp1* and $p19^{Arf}$ and $p16^{Ink4a}$ Taqman assays were custom-designed at ABI. Values were normalized to the expression of the *β-actin* internal reference. Average gene expression levels from three mice of each genotype were shown in bar graphs with standard errors. Statistical analyses were conducted by unpaired Student *t*-tests. The significance levels were shown in the number of stars, i.e., * was used for $0.01 < P < 0.05$, ** for $0.001 < P < 0.01$ and *** for $P < 0.001$.

Electrophoretic Mobility Shift Assay (EMSA) and chromatin immunoprecipitation

To confirm the binding of Dmp1 protein to the *Areg* promoter, EMSA was performed as described previously with recombinant Dmp1 protein prepared in Sf9 cells.6 In brief, the recombinant Dmp1 protein was incubated with an [α^{32}P]-labeled oligonucleotide probe covering the consensus sequence of the *Areg* promoter obtained by annealing the sense oligonucleotide 5′-TTTACCCCAGAACGGGATGGGGAGCAT-3′ and its reverse complementary sequence (Areg#1) (Figure 3*a*, top panel). The putative Dmp1-binding site is underlined. To demonstrate the direct binding of Dmp1 to the sequence located at the intron 1 of the *Areg* gene, EMSA was conducted with the oligonucleotide 5′-TTTGCTCAGGTGAGCATCCGCCACCTCTCAGG-3′ and its reverse complementary strand (Areg#2). To examine whether Dmp1 binds to the 3′ non-coding sequence of mouse thrombospondin-1 (*Tsp-1*) genomic DNA, oligonucleotide 5′-TTTCAGAGCCTGCGTATGTTATAACG-3′ and its reverse complementary strand (Tsp-1#1) were used (Figure 3*a*, the 2nd panel). To study if Dmp1 binds to the 3′ non-coding sequence of the mouse *JunB* genomic DNA, the oligonucleotide 5′-TTTTTTTCTTCCAAGCTGGGCGGATGGAGGGAGAAGATT G-3′ (JunB#1) and its reverse complementary strand was used (Figure 3*a*, the 3rd panel). To study whether Dmp1 binds to the mouse *Egr1* promoter, oligonucleotide 5′-TTTAAAACGAAGGTGGAGGCGGATGGAGAGAGAGAGAGAGAG-3′ and its reverse complementary strand (Egr1#1) were used (Figure 3*a*, the 4th panel). For control EMSA, the oligonucleotide 5′-TTTGAGCCCTGGGAGCCATCCGAGCGGCTTTCAACAGACC-3′ (JunB#2; Figure 3*a*, Supplementary figure 1) and its complementary sequence were used. For competition assays, a 100-fold excess of unlabeled oligonucleotide was added to the reaction mixtures before probe incubation. To verify the identityof the proteins in shifted complexes, reaction mixtures were incubated with control non-immune rabbit serum or with

antibodies specific to Dmp1 (RAX: [rabbit antibody project X] to Dmp1 amino acids 136–150, RAF [rabbit antibody project F] to Dmp1 amino acids 752–760, RAJ [rabbit antibody project J] to the DNA-binding domain of Dmp1).1,9 Chromatin immunoprecipitation for *Areg*, *Tsp1*, *JunB* and *Egr1* genomic loci was conducted with RAX, RAZ (rabbit antibody project Z to the Dmp1 amino acids 740–756),3 and RAD (rabbit antibody project D to the full-length His-tagged Dmp1) antibodies as described previously.10,11 For Areg #1, sense 5′-AGCAGCAAGGACAGAATGGAC-3′ and antisense 5′-GCTGGGAAAGGAGGCTGTAGT-3′; for Areg #2, sense 5′-GCTGTTGCTGCTGGTCTTAGG-3′ and antisense 5′-GTTTCCATCAGCTGGTCCTTG-3′; for Tsp-1#1, sense 5′-GAAAGCCCTACTGGTCCATCC-3′ and antisense 5′-TGCACCATCACCACATTTCTC-3′; for JunB#1, sense 5′-TGTGGAGAAGAAACACGCACT-3′ and antisense 5′-CCTGAAAGGAGCGAGCTACAA-3′; for Egr1#1, sense 5′-GGTGAGACACAGGTTTGGTCA-3′ and antisense 5′-GGGAGGTTACTCTTCGGCTCT-3′ were used. As a control, we amplified the sequence 1.8 kb downstream from the JunB#1 site with the sense primer 5′-GGACCCCAGAATAAGCAGAGG-3′ and antisense primer 5′-CTGAGAACGGGTGCTGGTTAG-3′.

Transfection of C10 cells and Actinomycin D treatment

Non-transformed mouse alveolar epithelial cell line C1019 was received from Dr. LM Anderson, NCI/NIH. C10 cells (5×10^5 cells per 60 mm dish/4 mL) were transfected with 4μg of pFLEX1-Dmp1 or empty vector and were harvested for RNA extraction at 48 hours after transfection (Figure 4*a*). For inhibition of *de novo* mRNA synthesis, cells were treated with 2μg/mL of Actinomycin D (Sigma) for 6 hours before harvest. The transfection efficiency was 30 – 70 % with Genejuice (Novagen, EMD Chemicals, Gibbstown, NJ) in C10 cells.

Quantitative primary transcript real-time PCR (qPT-PCR)

C10 cells were transiently transfected with pFLEX1-Dmp1 or empty vector and were harvested for RNA extraction at 24 and 48 hours (Figure 4*c*). qPT-PCR was conducted as previously described20. Specific primers for mouse *Areg* exon 4 - intron 4, *Tsp-1* exon 7-intron 7, *Egr1* exon 1 - intron 1 real-time PCR were custom-designed at ABI. The primer sequences will be available upon request.

Western blotting

Murine Areg, Tsp-1, JunB, Egr1, Ect2 and Actin proteins were detected by direct Western blotting with 80μg of the lung lysates from $Dmp1^{+/+}$, $Dmp1^{+/-}$ and $Dmp1^{-/-}$ mice. For detection of Dmp1 in murine lung tissues, immunoprecipitation (IP) - Western blotting was conducted by lysing the lungs in EBC buffer,1 immunopprecipitation of 250μg of lysate with 5 μg of RAZ antibody,3 followed by Western blotting with the RAX antibody9. IP-Western blotting was necessary since the Dmp1 protein levels are relatively low in the lungs, especially in $Dmp1^{+/-}$ mice. The Areg antibody (AF989) was purchased from R&D Systems (Minneapolis, MN). The antibodies for Tsp-1 (sc-12312), JunB (sc-8051), Egr1 (sc-101033), Ect2 (sc-1005), $p27^{kip1}$ (sc-1641) and Actin (sc-47778, sc-1616) were obtained from Santa Cruz Biotechnology (Santa Cruz Biotechnology, Santa Cruz, CA).

Immunohistochemistry

Sections of paraffin-embedded lung tissues from $Dmp1^{+/+}$, $Dmp1^{+/-}$ and $Dmp1^{-/-}$ mice in C57BL/6 background were mounted on immunohistochemistry slides. The paraffin was

removed by melting at 70°C for 30 min, followed by soaking in xylene substitute (Thermo Electron Corp., Pittsburgh, PA) and rehydrating through decreasing ethanol concentrations. Antigen retrieval was performed by boiling slides in DakoCytomation Antigen Retrieval solution (Dako, Carpinteria, CA).9 Slides were blocked in 1 % BSA/PBS, containing 25μg/ml serum from the same species as the secondary antibody. After incubating with primary and secondary antibodies, staining was visualized with an alkaline phosphatase or peroxidase-based detection kit (ABC kit; Vector Laboratories, Burlingame, CA), followed by hematoxylin counterstaining. Negative controls (incubation with secondary antibody only) for the immunohistochemical reactions were performed on serial sections.

Results

Expression profile from microarray analysis

To identify novel transcriptional target genes of Dmp1 that could account for tumor-prone phenotypes of *Dmp1*-deficient mice, GeneChip Microarray was performed using murine gene chip 430A. Out of 3,771 full-length known genes available in the gene chip, 127 genes (3.7 %) in the lung were upregulated at least 2-fold in $Dmp1^{-/-}$ mice in comparison to $Dmp1^{+/+}$ mice. In contrast, 104 genes in the lung (2.8 %) were downregulated a minimum of 2-fold in $Dmp1^{-/-}$ mice in comparison to $Dmp1^{+/+}$ mice. Among the total of 4,371 expressed sequence tags (ESTs), 0.5 % were upregulated at least 2-fold (data not shown). According to the gene functional analysis, the selected genes were further classified into different corresponding groups: cluster I, apoptosis and cytolysis; cluster II, cell surface receptor and signal transduction; cluster III, immune and inflammatory response; cluster IV, cell cycle, proliferation and transcription; and cluster V, metabolism and enzymes (Figure 1, Table 1).

Using high-throughput methodology, detection of multiple genes with their related cellular functions that might be involved in tumorigenesis in *Dmp1*-deficient mice is possible. Amphiregulin (*Areg*), adrenomedullin (*Adm*), *JunB, Egr1*, thrombospondin-1 (*Tsp-1*), *Bcl-3*, methyl DNA binding protein-1 (*Mbd1*), *Gas1* and *Ect2* were selected as candidate transcriptional target genes that contribute to the tumor-prone phenotype since these genes are involved in cell growth/differentiation (*Areg*, *Adm*, *Gas1* and *Ect2*), signal transduction/transcription (*JunB* and *Egr1*), angiogenesis/metastasis (*Tsp-1*), apoptosis (*Bcl-3*) or DNA methylation (*Mbd1*). These nine genes (hereafter called ‘novel Dmp1 targets’ or ‘novel Dmp1 target genes’) will be validated in later experiments.

Validation of microarray data by quantitative RT PCR

DNA microarray analysis measures expressional changes in thousands of transcripts and, therefore, the statistical evaluation of this data is prone to some errors. For this reason, we validated our initial microarray data by performing real-time RT-PCR (Figure 2). Results of the microarray analyses, real-time PCR and linear regression analyses demonstrated a strong correlation with Pearson’s correlation coefficient (*R*) of 0.931 for the lung (Figure 1*c*). In our study, the selected genes showed good correlation by real-time RT-PCR.

Expression of novel Dmp1 target genes in Dmp1-hetrozygous lungs

Published studies have shown that Dmp1 is haplo-insufficient for tumor suppression.13,14 Therefore, we examined relative expression levels of Dmp1 target genes in lungs with three different *Dmp1* genotypes (Figure 2). The statistically significant differences are shown in stars (* for $P < 0.05$, **for $0.001 < P < 0.05$ and *** for $P < 0.001$). The average *Dmp1* gene expression level in $Dmp1^{+/-}$ lungs was ~35 % of those in $Dmp1^{+/+}$ lungs, consistent with the result of our previous study (Figure 2*a*).14 The average *Arf* expression was downregulated to 14 % of wild-type levels in $Dmp1^{+/-}$ mice and 5 % in $Dmp1^{-/-}$ mice (Figure 2*b*). The

expression levels of the possible Dmp1 transcriptional target genes, *Areg*, *Tsp-1*, *JunB*, *Egr1* and *Adm* were downregulated to 10–25 % of wild-type levels in both $Dmp1^{+/-}$ and $Dmp1^{-/-}$ lungs, while *Bcl-3* and *Mbd1* were moderately downregulated to 30–50 % levels of those in wild-type lungs (Figure 2*c*–*i*).

We then studied the gene expression levels for *Gas1* and *Ect2*, the two genes showed to be upregulated in lung tissue from *Dmp1*-deficient mice, using GeneChip Microarray (Table 1). Both of these genes were upregulated three to four times in the lungs of $Dmp1^{+/-}$ and $Dmp1^{-/-}$ mice as shown Figure 2*j* and *k*. In contrast, $p27^{kip1}$ mRNA levels were no different among wild-type, $Dmp1^{+/-}$ and $Dmp1^{-/-}$ lungs (Figure 2*l*). In short, cancer-related, novel Dmp1 target gene expression levels were very similar between $Dmp1^{+/-}$ and $Dmp1^{-/-}$ lungs.

Dmp1 directly binds to the mouse Areg, Tsp-1, JunB and Egr1 genomic DNA

We then investigated whether Dmp1 directly binds to the promoters/enhancers of *Areg*, *Tsp-1*, *JunB* and *Egr1* since these genes were downregulated more than 80 % in *Dmp1*-deficient lungs. The mouse *Areg* promoter and the first intron have unique Dmp1-consensus sequences (#1: 5′-AACGGATGG and #2: 5′-GGCGGATGC [antisense]) (Figure 3*a*). EMSA conducted with recombinant Dmp1 proteins prepared in Sf9 cells show that the Dmp1 protein directly binds to the sequence #1 (Figure 3*b*, complex B). This complex was not antagonized by a 200-fold excess of non-specific oligos or with Ets-specific oligos (M3), but was antagonized by the cold probe. Complex B disappeared (RAJ) or was supershifted when the protein-probe mixture was incubated with specific antibody to the carboxyl terminus of Dmp1 (complex S1 with RAF) (Figure 3*b*). Thus, Dmp1 directly binds to the *Areg* promoter. Likewise, binding of Dmp1 to the intron 1 of *Areg* was confirmed (Figure 3*c*, complex C, supershifted at S2). For *Tsp-1*, EMSA was conducted with a [α^{32}P]-labeled probe covering the Dmp1-consensus sequence (5′-TGCGTATGT) located at the 3′ of exon 21 (Figures 3*a* and 3*d*). The complex D was specifically antagonized by cold probe and was interfered (RAX and RAJ) or supershifted (S3 with RAF) when incubated with antibodies to Dmp1 (Figure 3*d*). In *JunB*, Dmp1 bound to the genomic sequence 5′-GGCGGATGG (JunB#1) (Figures 3*a*, 3*e*), but not to the sequence 5′-CTCGGATGG (JunB#2, antisense) located at the 3′ region of the locus (Supplementary figure 1), showing specificity of Dmp1 binding to JunB#1. Direct binding of Dmp1 to the mouse *Egr1* promoter was also demonstrated by EMSA with supershift assays (complex F was shifted to S5; Figures 3*a*, 3*f*).

Binding of Dmp1 to the endogenous *Areg*, *Tsp-1*, *JunB* and *Egr1* genomic loci was verified by chromatin immunoprecipitation (ChIP) with three different antibodies to Dmp1 (Figure 3*g*). The specificity of Dmp1 binding to the target genes was confirmed by control PCR amplification of the sequence 1.8 kb downstream from the JunB#1 site (Figure 3*g*, JunB control). Although specific Dmp1 motifs used in EMSA may not account for the ChIP results, our data indicate that both recombinant and endogenous Dmp1 proteins bind to the genomic sequence on the *Areg*, *Tsp-1*, *JunB* and *Egr1* promoter/enhancer regions.

To demonstrate that these genes identified by GeneChip Microarray are regulated by Dmp1 at transcriptional levels, we transfected the murine alveolar Type II epithelial cell line C1019 with a Dmp1 expression vector and studied the expression levels by real-time PCR. *Areg*, *Tsp-1*, *JunB*, *Egr1*, *Bcl-3*, *Mbd1* and *Adm* transcripts were significantly upregulated (2–5 fold) (Figure 4*a*) in Dmp1-expressing cells while *Gas1* and *Ect2* gene expression was significantly repressed (30–40 %) (Figure 4*b*). On the other hand, the $p27^{kip1}$ gene expression did not change significantly on transient expression of Dmp1 (Figure 4*b*). These effects were completely abolished by simultaneous treatment of transfected cells with 2μg/mL Actinomycin D, a potent inhibitor of *de novo* mRNA synthesis (Figure 4*a*, *b*). In order

to confirm these results, we conducted quantitative primary transcript real-time PCR (qPT-PCR) analysis on *Areg*, *Tsp1* and *Egr1* genes that consists of 2 or more exons (Figure 4*c*). This assay measures the relative abundance of primary, un-spliced transcripts relative to those of mature RNA. Using *Areg* exon 4 - intron 4 and exon 4 - exon 5, *Tsp-1* exon 7-intron 7 and exon 7 - exon 8, *Egr1* exon 1 - intron 1 and exon 1- exon 2 primer pairs for qPT-PCR, the relative abundance of immature (pre) and mature *Areg*, *Tsp-1* and *Egr1* transcripts were similarly elevated at 24 and 48 hours in C10 cells transfected with the Dmp1 expression vector (Figure 4*c*). These results indicate that regulation of these target genes by Dmp1 occurs at transcriptional levels.

Areg, Tsp-1, JunB and Egr1 proteins are barely detectable in the lungs from Dmp1$^{+/-}$ and Dmp1$^{-/-}$ mice

To verify the results of the GeneChip Microarray and real-time PCR at protein levels, Western blotting was conducted using the lung lysates from the three different *Dmp1* genotypes. The levels of Areg, Tsp-1, JunB and Egr1 proteins were significantly downregulated in the lungs from *Dmp1*$^{-/-}$ and *Dmp1*$^{+/-}$ mice in comparison to wild-type tissues (Figure 5*a*). Conversely, the Ect2 protein was upregulated in the lungs from *Dmp1*$^{-/-}$ and *Dmp1*$^{+/-}$ mice (Figure 5*a*). Since detection of the Dmp1 protein in normal mouse lung was difficult by direct Western blotting, we performed immunoprecipitation - Western blotting using 250μg of cell lysates (Figure 5*b*). Interestingly, the expression of the 130 and 160 kDa bands for Dmp1 was significantly downregulated in the lungs of *Dmp1*$^{+/-}$ mice (10–20 % of wild-type levels) (Figure 5*b*, lanes 3–6). No specific bands were detectable with lysates from *Dmp1*$^{-/-}$ mice (Figure 5*b*, lanes 1, 2) or wild-type lung lysates immunoprecipitated with control IgG (lane 7). All these results are consistent with the findings of mRNA analysis by real-time PCR and explain the mechanism of haploid insufficiency of Dmp1.

To confirm the results of Western blotting and demonstrate the changes of Dmp1 and its target protein expression at a cellular level, immunohistochemical studies were conducted in the lungs from *Dmp1*-knockout mice with specific antibodies. We previously reported that murine lung tissue showed positive staining with antibody to Dmp1 (RAX) in the nuclei of alveolar macrophages and type II cells.9 We found significant downregulation of bronchial and alveolar Dmp1 signals in the lungs from *Dmp1*$^{+/-}$ mice in comparison to the wild-type lung, reflecting its mRNA levels (Supplementary figure 2*a–c*). Next, the lungs from mice of three different *Dmp1* genotypes were stained with antibodies to Areg, Tsp-1, JunB and Egr1 to confirm the downregulation of the target gene products in the lungs of *Dmp1*$^{+/-}$ and *Dmp1*$^{-/-}$ mice (Figure 6*a–i*; Supplemental figure 2*d–f*). Areg was expressed in alveolar macrophages, type II cells, and bronchial epithelial cells of a wild-type mouse (Figure 6*a*). The Areg signals were barely detectable in the lungs from mice with a *Dmp1*$^{+/-}$ or *Dmp1*$^{-/-}$ background (Figure 6*b*, *c*). This outcome is consistent with the results of Western blotting (Figures 5) and recapitulates the downregulation of *Areg* mRNA by real-time PCR (Figures 1, 2). The Tsp-1 staining was expressed in the bronchial epithelial cells and alveolar type II cells (Figure 6*d*). The cytoplasmic signals were significantly downregulated in the lungs from *Dmp1*$^{+/-}$ and *Dmp1*$^{-/-}$ mice (Figure 6*e*, *f*). Likewise, JunB was expressed in the nuclei of alveolar macrophages and alveolar type II cells (Figure 6*g*). These signals were barely detectable in the lung from *Dmp1*$^{+/-}$ or *Dmp1*$^{-/-}$ mice (Figure 6*h*, *i*).

We also confirmed upregulation of the Ect2 protein in the bronchial epithelium from *Dmp1*$^{+/-}$and *Dmp1*$^{-/-}$ mice in comparison to *Dmp1*$^{+/+}$ mice (Figure 6*j–l*). Upregulation of the Ect2 protein was also found in *K-ras*^{LA} lung tumors from *Dmp1*$^{-/-}$ and *Dmp1*$^{+/-}$ mice14 (Supplementary figure 3), suggesting that Ect2 overexpression may play critical roles in lung cancer development in *Dmp1*-deficient animals. In contrast, all of *Dmp1*$^{+/+}$, *Dmp1*$^{+/-}$ and *Dmp1*$^{-/-}$ lungs showed equal signals with p27^{kip1} antibody (Supplementary figure 2*g–i*)

and cytoplasmic staining with Actin antibody (Figure 6*m–o*). Thus, our Western blotting and immunohistochemical studies are consistent with the results of GeneChip Microarray and real-time PCR for novel Dmp1 target genes.

Discussion

Dmp1 demonstrates its activity as a tumor suppressor through the activation of the Arf-Mdm2-p53 pathway. In this study, we have identified a number of novel target genes for Dmp1 that are involved in cell proliferation/differentiation, signal transduction/transcription, angiogenesis/metastasis, or apoptosis through GeneChip Microarray of mouse lung tissues. The results were verified by real-time PCR, Western blotting, immunohistochemistry and by expressing Dmp1 in non-transformed alveolar epithelial cells. Inhibition of novel mRNA synthesis nullified the effects of Dmp1 in lung epithelial cells, demonstrating that the gene regulation by Dmp1 occurred at transcriptional levels. Direct binding of Dmp1 to the genomic loci of *Areg*, *Tsp-1*, *JunB* and *Egr1* indicates that these are direct transcriptional targets for Dmp1.

Among the identified genes, we chose to focus our attention on a small subset due to their involvement in cell proliferation and differentiation. For example, Areg, one of the ligands of the EGF family,[21–23] promotes the growth of carcinoma cells, keratinocytes and normal lung epithelial cells in the presence of extracellular matrix,[22] but inhibits the growth of some transformed cell lines and lung epithelial cells in the absence of extracellular matrix.[22,23] Thus, Areg can either stimulate or inhibit the growth of lung cancer cells, dependent on the biological settings. It has recently been reported that brain metastasis of NSCLC is associated with higher expression of Areg protein in tumor cells.[24] It was also shown that high circulating Areg is linked to progressive disease of NSCLC.[25] Therefore, Areg is considered to be a growth promoting factor in human NSCLC. If NSCLC that shows LOH for h*DMP1* is associated with low Areg expression, the patients may have a less aggressive disease and thus will have a favorable prognosis. This prediction is consistent with our recent study where we showed mutually exclusive inactivation of h*DMP1* and *INK4a/ARF* or *p53* in NSCLC since the latter two groups are associated with poor prognosis of patients.[3] Further studies with clinical samples will be required to demonstrate the correlation between deletion of h*DMP1*, expression of Areg, and survival of patients in human NSCLC.

Our microarray data indicate that Tsp-1 is significantly downregulated in the $Dmp1^{-/-}$ lung (to 10–15 %). Tsp-1 in the alveolar epithelial cells and macrophages were barely detectable in the lungs from $Dmp1^{-/-}$ mice in immunohistochemical studies, and our EMSA studies demonstrate the direct binding of Dmp1 to the genomic locus of *Tsp-1*, indicating that Dmp1 is a critical regulator of *Tsp-1*. Tsp-1 is an endogenous inhibitor of angiogenesis, which limits blood vessel density in normal tissues and restrains tumor growth.[26–28] Recent studies demonstrated that in the absence of *Tsp-1*, proangiogenic signaling is enhanced, possibly through up-regulation of fibronectin expression. The enhanced signaling further promotes endothelial cell proliferation, migration and survival.[27,28] Since Tsp-1 levels are very low in both $Dmp1^{+/-}$ and $Dmp1^{-/-}$ lungs, it is expected that lung cancers from *Dmp1*-knockout mice will exhibit a more invasive and metastatic phenotypes than those from $Dmp1^{+/+}$ mice. Indeed, we recently found that *K-ras*^{LA}-induced lung tumors from $Dmp1^{+/-}$ or $Dmp1^{-/-}$ mice often showed signs of intrabronchial and intravascular invasion in comparison to the $Dmp1^{+/+}$ lung tumors of the same age.[14] Thus, Dmp1 prevents tumor formation by simultaneously activating the Arf-p53 pathway and by preventing angiogenesis by upregulating Tsp-1.

Our results show significant downregulation of *JunB* in the lung of $Dmp1^{-/-}$ mice versus wild-type. These results were confirmed by real-time PCR and immunohistochemistry. We

previously reported that the *Dmp1* promoter was activated by oncogenic Ras and activation of the *Dmp1* promoter was strikingly impaired in c-*Jun* or *JunB*-knockdown cells.10 Thus, Jun proteins play critical roles in *Dmp1* promoter activation by oncogenic Ras. It is generally considered that JunB is a negative regulator of proliferation.29,30 JunB prevents G1-S phase transition by simultaneously activating $p16^{INK4a}$ and repressing *cyclin D1* transcription.30 Although Dmp1 has been shown to be a physiological regulator of $p19^{Arf}$, it may regulate the transcription of $p16^{Ink4a}$ as well indirectly through the upregulation of *JunB*. Indeed, we noticed that the $p16^{Ink4a}$ mRNA was significantly downregulated (to 18 %) in the lungs from $Dmp1^{-/-}$ mice in comparison to wild-type littermates (data not shown). Thus, *JunB* is located both upstream and downstream of the Dmp1 signaling, collectively contributing to tumor suppression.

Another intriguing Dmp1 target gene identified in this study is *Egr1*. Egr1 is a zinc-finger transcription factor and activates transcription as a monomer. It has been reported that Egr1 shows tumor suppressor activities through induction of TGFβ1 and direct induction of *p53* and *PTEN*31. In human NSCLC, low levels of Egr1 expressions are associated with poor outcome and resistance to therapy32. Since *Egr1* is a direct transcriptional target of Dmp1, it is very likely that *Dmp1* deletion leads to lung cancer development by lowering *Egr1* levels. Of note, Tschan *et al.* recently showed that the WT1, which has significant structural homology with Egr1, repressed the h*DMP1* promoter through direct binding to the Egr1/Sp1 site.12 Thus, it is possible that Egr1, like JunB, is located both upstream and downstream of the Dmp1 signaling, both contributing to tumor suppression.

The current DNA microarray and quantitative RT-PCR analyses not only revealed the down-regulation of *Areg, Tsp-1, JunB, Egr1, Adm*33–35, *Bcl-3*36–38 and *Mbd1*39–41, but also showed significant upregulation of growth arrest-specific 1 (*Gas1*, 5.40 in the lung)42, *Ect2*43–45 and other transcripts in $Dmp1^{-/-}$ mice. Chalamalasetty *et al.* showed that nucleotide-exchange factor Ect2 localized to the central spindle and to the cell cortex in mitotic cells.44 Depletion of Ect2 impaired cleavage furrow formation and RhoA and Citron kinase failed to accumulate at the cleavage furrow, suggesting that Ect 2 is essential for cytokinesis.44 Hirata *et al.* conducted tumor tissue microarray and showed that a high level of ECT2 expression was associated with poor prognosis for patients with NSCLC.45 They also showed that knocking down of *ECT2* expression by small interfering RNAs effectively suppressed lung cancer cell growth, suggesting specific role of ECT2 in lung cancer development.45 Interestingly, Ect2 protein was significantly upregulated in the lungs from $Dmp1^{-/-}$; $K\text{-}ras^{LA}$ mice, suggesting that increased Ect2 expression caused by *Dmp1* loss contributes lung tumor development. Since LOH of h*DMP1* is found in ~35 % of human NSCLC14 and Dmp1 is a negative regulator for Ect2, it will be imperative to study the correlation of *h*DMP1 and ECT2 expression in human NSCLC samples and determine the prognostic value of h*DMP1*-loss in human NSCLC.3

Dmp1 has been shown to be haplo-insufficient for tumor suppression.2,3,13,14 It has been reported that loss of one *p53* allele results in a four-fold reduction of p53 mRNA and protein levels, which could explain the mechanisms of haplo-insufficiency of p53 in tumor suppression.46 Interestingly, our study also showed that the *Dmp1* mRNA levels in $Dmp1^{+/-}$ lungs were ~35 % of those in $Dmp1^{+/+}$ lungs; the Dmp1 protein levels were even lower (10–20 % of wild-type) in the lungs from $Dmp1^{+/-}$ mice. Consistently, all the nine cancer-related Dmp1 target genes (including $p19^{Arf}$) that were downregulated in $Dmp1^{-/-}$ lungs were also repressed in $Dmp1^{+/-}$ lungs. Likewise, both *Gas1* and *Ect2* genes that were upregulated in $Dmp1^{-/-}$ lungs were highly expressed in $Dmp1^{+/-}$ tissues, indicating that cancer-related gene expression is very close between $Dmp1^{+/-}$ and $Dmp1^{-/-}$ lungs. These data were further confirmed by immunohistochemistry with specific antibodies. EMSA showed direct binding of Dmp1 to *Areg*, *Tsp-1*, *JunB* and *Egr1*, and overexpression of

Dmp1 induced either upregulation or downregulation of novel Dmp1 target genes in non-transformed alveolar epithelial cells. Although the detailed molecular mechanisms for unexpectedly low Dmp1 protein expression in *Dmp1*$^{+/-}$ lungs remain to be determined, this study not only identified novel genes that are regulated by Dmp1, but also gave insights into the mechanisms of haploid insufficiency of Dmp1 in tumor suppression.

In summary, we performed a rigorous genome-wide examination of genes with expressional changes specifically associated with *Dmp1*. We found numerous genes that regulate cell growth and are downstream targets of the Dmp1 transcription factor. Interestingly, many of these are involved in the signaling pathways that regulate Dmp1. We also identified *Tsp-1* as a novel target for Dmp1, which plays critical roles in the prevention of tumor angiogenesis and metastasis. Although transcriptional repressor function of Dmp1 has never been reported, significant subsets of genes were upregulated in *Dmp1*$^{-/-}$ lung in this study. The current findings are highly worthy of further investigation to elucidate the function of Dmp1, which is located at the cusp of oncogenic and tumor suppressor signal transduction.

Supplementary Material

Refer to Web version on PubMed Central for supplementary material.

Acknowledgments

We thank Lou Craddock and Elizabeth Fry for their technical assistance. We are grateful to Dr. Lucy Anderson for C10 cells, Drs. Charles Sherr and Martine Roussel for reagents and transfer of *Dmp1*-null mice, Dr. Emmanuelle Passague for sharing unpublished data, and Ms. Karen Klein for editing. This work was supported by NIH/NCI 5R01CA106314, American Cancer Society RSG-07-207-01-MGO, and by a Wake Forest University Comprehensive Cancer Center multi-investigator grant P30CA12197 GAC (all for K. Inoue). P. Taneja is supported by the Susan G. Komen Foundation postdoctoral fellowship KG080179.

References

1. Hirai H, Sherr CJ. Interaction of D-type cyclins with a novel myb-like transcription factor, DMP1. Mol Cell Biol. 1996; 16:6457–67. [PubMed: 8887674]
2. Sugiyama T, Frazier DP, Taneja P, Kendig RD, Morgan RL, Matise LA, Lagedrost SJ, Inoue K. Signal transduction involving the Dmp1 transcription factor and its alteration in human cancer. Clinical Medicine: Oncology. 2008; 2:209–19.
3. Sugiyama T, Frazier DP, Taneja P, Morgan RL, Willingham MC, Inoue K. The role of Dmp1 and its future in lung cancer diagnostics. Expert Rev Mol Diagn. 2008; 8:435–48. [PubMed: 18598225]
4. Inoue K, Sherr CJ. Gene expression and cell cycle arrest mediated by transcription factor DMP1 is antagonized by D-type cyclins through a cyclin-dependent-kinase-independent mechanism. Mol Cell Biol. 1998; 18:1590–600. [PubMed: 9488476]
5. Inoue K, Sherr CJ, Shapiro LH. Regulation of the CD13/aminopeptidase N gene by DMP1, a transcription factor antagonized by D-type cyclins. J Biol Chem. 1998; 273:29188–94. [PubMed: 9786929]
6. Inoue K, Roussel MF, Sherr CJ. Induction of ARF tumor suppressor gene expression and cell cycle arrest by transcription factor DMP1. Proc Natl Acad Sci USA. 1999; 96:3993–8. [PubMed: 10097151]
7. Seth A, Watson DK. ETS transcription factors and their emerging roles in human cancer. Eur J Cancer. 2005; 41:2462–78. Review. [PubMed: 16213704]
8. Inoue K, Wen R, Rehg JE, Adachi M, Cleveland JL, Roussel MF, Sherr CJ. Disruption of the ARF transcriptional activator DMP1 facilitates cell immortalization, Ras transformation, and tumorigenesis. Genes Dev. 2000; 14:1797–809. [PubMed: 10898794]
9. Mallakin A, Taneja P, Matise LA, Willingham MC, Inoue K. Expression of Dmp1 in specific differentiated, nonproliferating cells and its regulation by E2Fs. Oncogene. 2006; 25:7703–13. [PubMed: 16878159]

10. Sreeramaneni R, Chaudhry A, McMahon M, Sherr CJ, Inoue K. Ras-Raf-Arf signaling critically depends on the Dmp1 transcription factor. Mol Cell Biol. 2005; 25:220–32. [PubMed: 15601844]
11. Taneja P, Mallakin A, Matise LA, Frazier DP, Choudhary M, Inoue K. Repression of Dmp1 and the Arf transcription by anthracyclins: critical roles of the NF-κB subunit p65. Oncogene. 2007; 26:7457–66. [PubMed: 17546045]
12. Tschan MP, Gullberg U, Shan D, Torbett BE, Fey MF, Tobler A. The hDMP1 tumor suppressor is a new WT1 target in myeloid leukemias. Leukemia. 2008; 22:1087–90. [PubMed: 17972942]
13. Inoue K, Zindy F, Randle DH, Rehg JE, Sherr CJ. Dmp1 is haplo-insufficient for tumor suppression and modifies the frequencies of Arf and p53 mutations in Myc-induced lymphomas. Genes Dev. 2001; 15:2934–9. [PubMed: 11711428]
14. Mallakin A, Sugiyama T, Taneja P, Matise LA, Frazier DP, Choudhary M, Hawkins GA, D'Agostino RB Jr, Willingham MC, Inoue K. Mutually exclusive inactivation of DMP1 and ARF/p53 in lung cancer. Cancer Cell. 2007; 12:381–94. [PubMed: 17936562]
15. Brown PO, Botstein D. Exploring the new world of the genome with DNA microarrays. Nature Genet. 1999; 21:33–7. [PubMed: 9915498]
16. Lipshutz RJ, Fodor SPA, Gingeras TR, Lockhart DJ. High density synthetic oligonucleotide arrays. Nature Genet. 1999; 21:20–4. [PubMed: 9915496]
17. Mallakin A, Kutcher LW, McDowell SA, Kong S, Schuster R, Lentsch AB, Aronow BJ, Leikauf GD, Waltz SE. Gene expression profiles of Mst1r-deficient mice during nickel-induced acute lung injury. Am J Respir Cell Mol Biol. 2006; 34:15–27. [PubMed: 16166746]
18. Lockhart DJ, Dong H, Byrne MC, Follettie MT, Gallo MV, Chee MS, Mittmann M, Wang C, Kobayashi M, Horton H, Brown EL. Expression monitoring by hybridization to high-density oligonucleotide arrays. Nat Biotechnol. 1996; 14:1675–80. [PubMed: 9634850]
19. Kammouni W, Ramakrishna G, Sithanandam G, Smith GT, Fornwald LW, Masuda A, Takahashi T, Anderson LM. Increased K-ras protein and activity in mouse and human lung epithelial cells at confluence. Cell Growth Differ. 2002; 13:441–8. [PubMed: 12354753]
20. Keller UB, Old JB, Dorsey FC, Nilsson JA, Nilsson L, MacLean KH, Chung L, Yang C, Spruck C, Boyd K, Reed SI, Cleveland JL. Myc targets Cks1 to provoke the suppression of p27Kip1, proliferation and lymphomagenesis. EMBO J. 2007; 26:2562–74. [PubMed: 17464290]
21. Polosa R, Prosperini G, Leir SH, Holgate ST, Lackie PM, Davies DE. Expression of c-erbB receptors and ligands in human bronchial mucosa. Am J Respir Cell Mol Biol. 1999; 20:914–23. [PubMed: 10226061]
22. Schuger L, Johnson GR, Gilbride K, Plowman GD, Mandel R. Amphiregulin in lung branching morphogenesis: interaction with heparan sulfate proteoglycan modulates cell proliferation. Development. 1996; 122:1759–67. [PubMed: 8674415]
23. Shoyab M, McDonald VL, Bradley JG, Todaro G. Amphiregulin, a bifunctional growth-stimulating glycoprotein produced by the phorbol 12-myristate 13 acetate-treated human breast adenocarcinoma cell line MCF-7. Proc Natl Acad Sci USA. 1988; 85:6528–32. [PubMed: 3413110]
24. Sun M, Behrens C, Feng L, Ozburn N, Tang X, Yin G, Komaki R, Varella-Garcia M, Hong WK, Aldape KD, Wistuba II. HER family receptor abnormalities in lung cancer brain metastases and corresponding primary tumors. Clin Cancer Res. 2009; 15:4829–37. Epub 2009 Jul 21. [PubMed: 19622585]
25. Masago K, Fujita S, Hatachi Y, Fukuhara A, Sakuma K, Ichikawa M, Kim YH, Mio T, Mishima M. Clinical significance of pretreatment serum amphiregulin and transforming growth factor-alpha, and an epidermal growth factor receptor somatic mutation in patients with advanced non-squamous, non-small cell lung cancer. Cancer Sci. 2008; 99:2295–301. Epub 2008 Sep 22. [PubMed: 18811692]
26. Lawler J, Sunday M, Thibert V, Duquette M, George EL, Rayburn H, Hynes RO. Thrombospondin-1 is required for normal murine pulmonary homeostasis and its absence causes pneumonia. J Clin Invest. 1998; 101:982–92. [PubMed: 9486968]
27. Jimenez B, Volpert OV, Crawford SE, Febbraio M, Silverstein RL, Bouck N. Signals leading to apoptosis-dependent inhibition of neovascularization by thrombospondin-1. Nat Med. 2000; 6:41–8. [PubMed: 10613822]

28. Folkman J. Angiogenesis: an organizing principle for drug discovery? Nature Rev Drug Disc. 2007; 6:273–86.
29. Shaulian E, Karin M. AP-1 as a regulator of cell life and death. Nat Cell Biol. 2002; 4:E131–6. [PubMed: 11988758]
30. Bakiri L, Lallemand D, Bossy-Wetzel E, Yaniv M. Cell cycle-dependent variations in c-Jun and JunB phosphorylation: a role in the control of cyclin D1 expression. EMBO J. 2000; 19:2056–68. [PubMed: 10790372]
31. Baron V, Adamson ED, Calogero A, Ragona G, Mercola D. The transcription factor Egr1 is a direct regulator of multiple tumor suppressors including TGFbeta1, PTEN, p53, and fibronectin. Cancer Gene Ther. 2006; 13:115–24. [PubMed: 16138117]
32. Ferraro B, Bepler G, Sharma S, Cantor A, Haura EB. EGR1 predicts PTEN and survival in patients with non-small-cell lung cancer. J Clin Oncol. 2005; 23:1921–26. [PubMed: 15774784]
33. Hinson JP, Kapas S, Smith DM. Adrenomedullin, a multifunctional regulatory peptide. Endocrine Rev. 2007; 21:138–67. [PubMed: 10782362]
34. Martinez A, Miller MJ, Unsworth EJ, Siegfried JM, Cuttitta F. Expression of adrenomedullin in normal human lung and in pulmonary tumors. Endocrinology. 1995; 136:4099–105. [PubMed: 7649118]
35. Zudaire E, Martinez A, Cuttitta F. Adrenomedullin and cancer. Regul Pept. 2003; 112:175–83. [PubMed: 12667640]
36. Courtois G, Gilmore TD. Mutations in the NF-κB signaling pathway: implications for human disease. Oncogene. 2006; 25:6831–43. [PubMed: 17072331]
37. Hayden MS, Ghosh S. Shared principles in NF-kappaB signaling. Cell. 2008; 132:344–62. [PubMed: 18267068]
38. Martin-Subero JI, Wlodarska I, Bastard C, Picquenot JM, Hoppner J, Giefing M, Klapper W, Siebert R. Chromosomal rearrangements involving the BCL3 locus are recurrent in classical Hodgkin and peripheral T-cell lymphoma. Blood. 2006; 108:401–2. [PubMed: 16790585]
39. Boyes J, Bird A. DNA methylation inhibits transcription indirectly via a methyl-CpG binding protein. Cell. 1991; 64:1123–34. [PubMed: 2004419]
40. Fujita N, Takebayashi S, Okumura K, Kudo S, Chiba T, Saya H, Nakao M. Methylation-mediated transcriptional silencing in euchromatin by methyl-CpG binding protein MBD1 isoforms. Mol Cell Biol. 1999; 19:6415–26. [PubMed: 10454587]
41. Meehan RR, Lewis JD, McKay S, Kleiner EL, Bird AP. Identification of a mammalian protein that binds specifically to DNA containing methylated CpGs. Cell. 1989; 58:499–507. [PubMed: 2758464]
42. Schneider C, King RM, Philipson L. Genes specifically expressed at growth arrest of mammalian cells. Cell. 1988; 54:787–93. [PubMed: 3409319]
43. Petronczki M, Glotzer M, Kraut N, Peters JM. Polo-like kinase 1 triggers the initiation of cytokinesis in human cells by promoting recruitment of the RhoGEF Ect2 to the central spindle. Dev Cell. 2007; 12:713–25. [PubMed: 17488623]
44. Chalamalasetty RB, Hummer S, Nigg EA, Sillje HH. Influence of human Ect2 depletion and overexpression on cleavage furrow formation and abscission. J Cell Sci. 2006; 119(Pt 14):3008–19. [PubMed: 16803869]
45. Hirata D, Yamabuki T, Miki D, Ito T, Tsuchiya E, Fujita M, Hosokawa M, Chayama K, Nakamura Y, Daigo Y. Involvement of epithelial cell transforming sequence-2 oncoantigen in lung and esophageal cancer progression. Clin Cancer Res. 2009; 15:256–66. [PubMed: 19118053]
46. Lynch CJ, Milner J. Loss of one p53 allele results in four-fold reduction of p53 mRNA and protein: a basis for p53 haplo-insufficiency. Oncogene. 2006; 25:3463–70. [PubMed: 16449974]

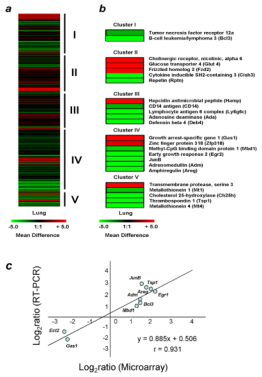

Figure 1.

Hierarchical clustering analysis of the 150 genes (displayed vertically) in the lung of *Dmp1*$^{+/+}$ and *Dmp1*$^{-/-}$ tissue samples. **(*a*)** The total 150 genes were clustered based on their expression patterns among the selected tissue samples. Cluster I, apoptosis and cytolysis genes; cluster II, cell surface receptor and signal transduction genes; cluster III, immune and inflammatory response genes; cluster IV, cell cycle/proliferation/transcription factor genes; and cluster V, genes for metabolism and enzymatic reactions. **(*b*)** Expression patterns of selected genes in five groups based on their functional classification (see Table 1 for their corresponding classification). Colored bars indicate relative expression levels. Red indicates upregulated genes in *Dmp1*$^{-/-}$; downregulated genes in *Dmp1*$^{-/-}$ mice are shown in green. Genes that are expressed at higher levels are assigned progressively brighter shades of red, whereas genes expressed at low levels are assigned shades of green. **(*c*)** Correlation of DNA microarray data and TaqMan RT-PCR assays. Total RNA was isolated from the lungs of *Dmp1*$^{+/+}$ and *Dmp1*$^{-/-}$ mice. A representative of three separate TaqMan RT-PCR experiments, all with similar results, is shown. Real-time PCR data were normalized for levels of *β-actin*. The fold changes obtained by both methods were log-transformed and the values were plotted against each other to evaluate their correlation. Selected genes are shown for illustrative purposes.

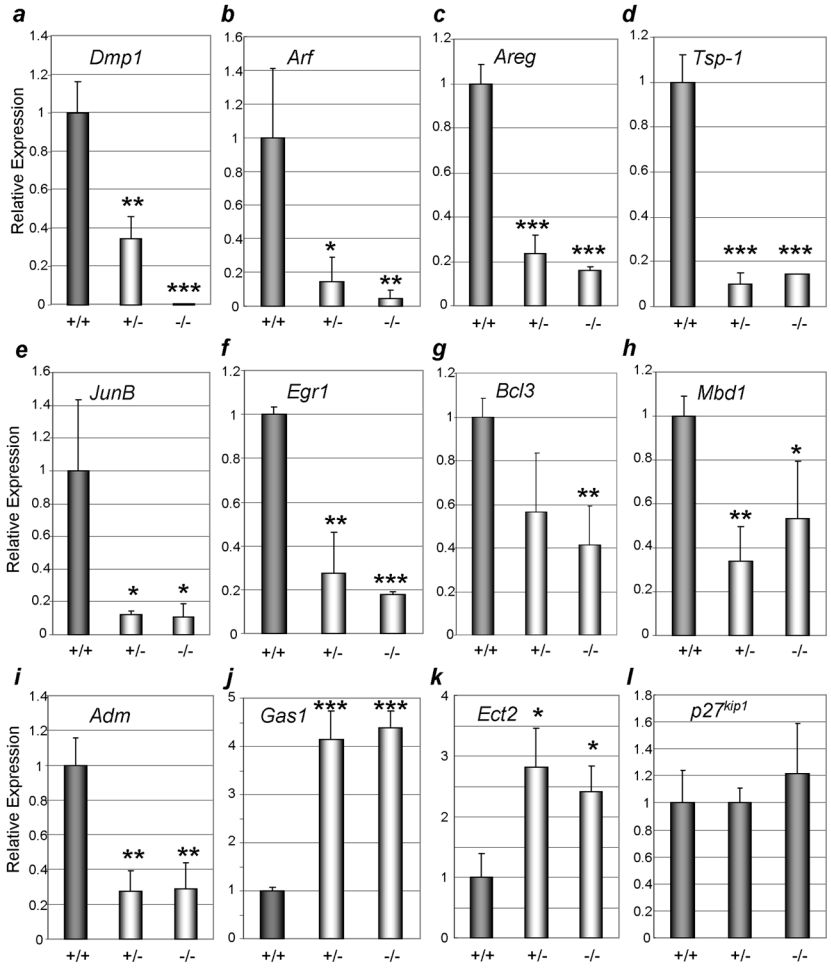

Figure 2.

Real-time RT-PCR analyses of target gene expression in the lungs from *Dmp1*$^{+/+}$, *Dmp1*$^{+/-}$ and *Dmp1*$^{-/-}$ mice. RNA was extracted from three mice of each *Dmp1* genotype (C57BL/6, 8–12 weeks old males) and gene expression was examined by real-time Taqman assay. The *Dmp1* gene was downregulated to 35 % of wild-type levels in *Dmp1*$^{+/-}$ lungs. It should be noted that novel Dmp1 target gene expression levels were not significantly different between *Dmp1*$^{+/-}$ and *Dmp1*$^{-/-}$ lungs, suggesting the mechanism of haploid insufficiency of Dmp1 for tumor suppression.

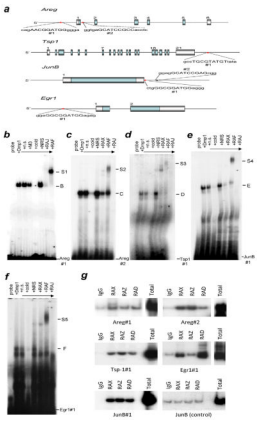

Figure 3.

Dmp1 directly binds to *Areg*, *Tsp-1*, *JunB* and *Egr1* loci. **(*a*)** Genomic structure of the murine *Areg*, *Tsp-1*, *JunB* and *Egr1* loci. The non-coding regions are shown in white and the coding regions are shown in blue. Top panel. There are two possible Dmp1-sites in the *Areg* promoter and in the first intron. The second panel. The murine *Tsp-1* locus. The Dmp1 consensus sequence is located at the 3′ of the *Tsp-1* gene. The third panel. The murine *JunB* locus. *JunB* is a single exon gene. The Dmp1 consensus sequence (JunB#1) is located in the 3′ region of the *JunB* gene. JunB#2 shows the position of the oligonucleotide sequence used for the control EMSA. The fourth panel. The murine *Egr1* locus. The *Egr1* gene consists of 2 exons and the Dmp1 motif is located 2 kb from the transcription initiation site. ***(b–f)*** EMSA was conducted with a [α^{32}P]-labeled probe covering possible Dmp1-consensus sequences, using recombinant Dmp1 protein prepared in Sf9 cells. The probes were: **(*b*)** Areg#1 within the *Areg* promoter, **(*c*)** Areg #2 within the first intron, **(*d*)** Tsp-1#1 at the 3′ of the locus, **(*e*)** JunB#1 at the 3′ of the locus and ***(f)*** Egr1#1 in the *Egr1* promoter. Competition assays were conducted with 100-fold excess scrambled oligos (n.s.), Ets-specific oligos (M3),1 or the cold probe itself. Supershift assays were conducted with control normal rabbit serum (NRS) or with three different antibodies to Dmp1 (RAX [to the peptide 136–150 at the DNA-binding domain], RAJ [to the DNA-binding domain] or RAF [to the peptide 752–760 at the C-terminus]).1›9 ***(g)*** Chromatin immunoprecipitation demonstrating the binding of endogenous Dmp1 to the *Areg*, *Tsp-1*, *JunB* and *Egr1* genomic loci. RAZ antibody recognizes the Dmp1 peptide 740–756,5 RAD antibody recognizes the full-length His-tagged Dmp1 protein. Total: total input chromatin corresponding to 4 % of the precipitated samples.

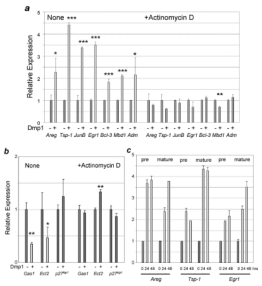

Figure 4.

Dmp1 regulates target gene expression in a non-transformed murine alveolar epithelial cell line, C10. C10 cells were transfected with pFLEX1-Dmp1 vector or control vector and mRNA levels were quantitated 48 hours after transfection by real-time RT-PCR. **(*a*)** Induction of *Areg*, *Tsp-1*, *JunB*, *Egr1*, *Bcl-3*, *Mbd1* and *Adm* genes by Dmp1. These gene inductions were nullified by Actinomycin D treatment, suggesting that Dmp1 increased the mRNA levels by transcriptional activation. **(*b*)** Repression of the *Gas1* and *Ect2* genes by Dmp1. This gene repression was also neutralized by Actinomycin D treatment, suggesting that the repression occurred at the transcriptional level. The $p27^{kip1}$ gene, which did not show any significant change in the GeneChip Microarray, was not affected by Dmp1 overexpression in C10 cells. ***(c)*** Primary quantitative primary transcript real-time PCR (qPT-PCR) analysis on *Areg*, *Tsp1* and *Egr1* genes. The relative abundance of immature (pre) and mature *Areg*, *Tsp-1* and *Egr1* transcripts were similarly elevated at 24 and 48 hours in C10 cells transfected with the Dmp1 expression vector.

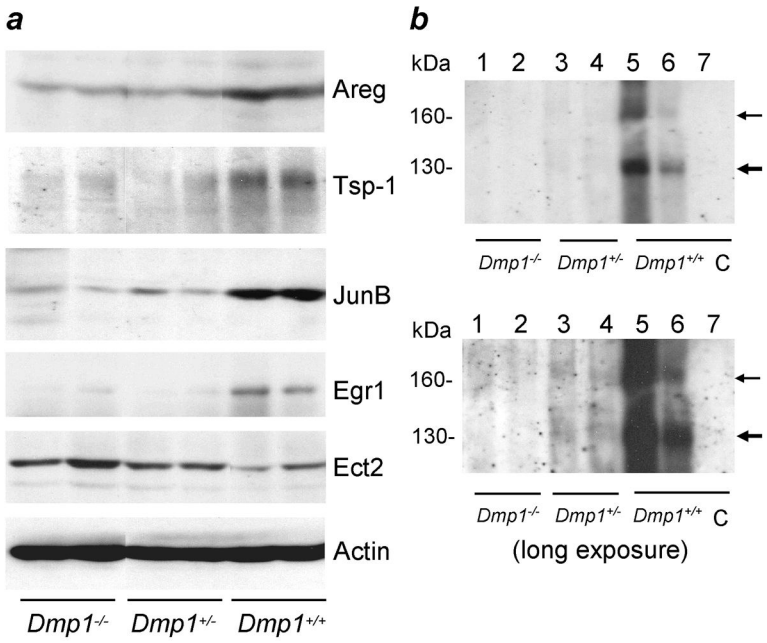

Figure 5.

Western blotting analysis of Dmp1, Areg, Tsp-1, JunB, Egr1, Ect2 and Actin proteins in the lungs from *Dmp1*$^{+/+}$, *Dmp1*$^{+/-}$ and *Dmp1*$^{-/-}$ mice. **(*a*)** Areg, Tsp-1, JunB and Egr1 proteins were downregulated in the lungs from *Dmp1*$^{+/-}$ and *Dmp1*$^{-/-}$ mice while the Ect2 protein was upregulated. **(*b*)** Immunoprecipitation (IP) - Western blotting analysis of Dmp1 expression in the lungs from *Dmp1*$^{+/+}$, *Dmp1*$^{+/-}$ and *Dmp1*$^{-/-}$ mice. The Dmp1 protein was not detectable in the lungs from *Dmp1*$^{-/-}$ mice and the expression of both 160 and 130 kDa Dmp1 proteins in the lungs from *Dmp1*$^{+/-}$ mice was decreased to 10–20 % of levels of wild-type tissue. C: Control immunoprecipitation of the wild-type lung lysate with rabbit IgG.

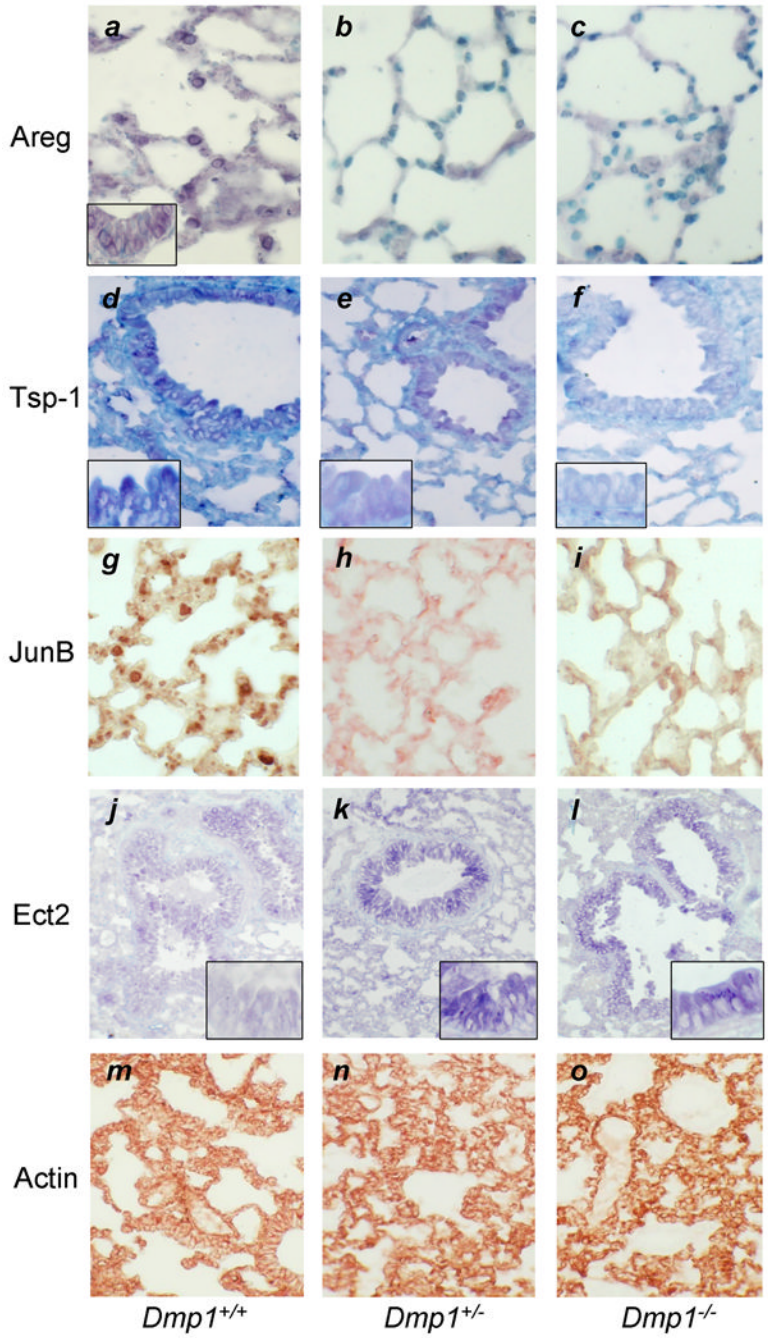

Figure 6.

Detection of Areg, Tsp-1, JunB, Ect2 and Actin proteins in wild-type, $Dmp1^{+/-}$ and $Dmp1^{-/-}$ lungs by immunohistochemistry. Magnification, ×40 in ***(a)–(i)***, ×20 in ***(j)–(o)***. **(*a*)** Areg is mainly stained in the cytoplasm of alveolar type II cells. The inset shows the expression of Areg in bronchial epithelial cells (×100). **(*b*), (*c*)** The Areg signal was significantly downregulated in both $Dmp1^{+/-}$ and $Dmp1^{-/-}$ lungs. **(*d*)** Tsp-1 staining is localized to the cytoplasm of normal bronchial epithelial cells and alveolar cells. The insets show the expression of Tsp-1 in bronchial epithelial cells (×100). **(*e*), (*f*)** The Tsp-1 signal was significantly downregulated in the lungs of $Dmp1^{+/-}$ and $Dmp1^{-/-}$ mice. **(*g*), (*h*), (*i*)** The JunB signal was found in the nuclei of alveolar type I and type II cells and macrophages

in wild-type mice, but not in the lungs of $Dmp1^{+/-}$, $Dmp1^{-/-}$ mice. **(*j*), (*k*), (*l*)** Upregulation of the Ect2 protein from $Dmp1^{+/-}$ and $Dmp1^{-/-}$ mice. The insets show the signals from bronchial epithelial cells (×100). **(*m*), (*n*), (*o*)** Staining with the β-Actin antibody in the lungs of $Dmp1^{+/+}$, $Dmp1^{+/-}$ and $Dmp1^{-/-}$ mice showing no significant difference among the three genotypes. The lung tissues were stained with alkaline phosphatase for panels ***(a)*–*(f)*** and ***(j)*–*(l)***; peroxidase for panels ***(g)*–*(i)*** and ***(m)*–*(o)***.

Table 1

Gene Name	Genebank	*Dmp1*$^{+/+}$ vs. *Dmp1*$^{-/-}$ (Lung)
Apoptosis and Cytolysis		
Tumor necrosis factor receptor superfamily, member 12a (Tnfrsf12a)	NM_013749	−2.54
B-cell leukemia/lymphoma 3 (Bcl3)	NM_033601	−3.18
Cell Surface Receptor and Signal Transduction		
Cholinergic receptor, nicotinic, alpha polypeptide 6	AW048864	7.16
Chloride channel calcium activated 3 (Clca3)	NM_017474	6.94
Cystic fibrosis transmembrane conductance regulator (cftr11MT1)	X72693	6.36
Potassium voltage-gated channel, shaker-related subfamily, member 5 (Kcna5)	NM_008419	4.50
Glucose transporter 4 (Glut4)	AB008453	3.80
Frizzled homolog 2 (Fzd2)	BB371406	3.58
Septin 6 (Sept 6)	BG920446	2.48
Breast cancer anti-estrogen resistance 3 (Bcar3)	NM_013867	−2.06
Tumor-associated antigen 1 (Taa1)	NM_009310	−2.14
Plasminogen activator urokinase receptor (Plaur)	X62701	−2.34
Loricrin (Lor)	NM_008508	−2.80
Cytokine inducible SH2-containing protein 3 (Cish3)	BB241535	−3.58
Repetin (Rptn)	NM_009100	−4.64
Immune and Inflammatory Response		
Hepcidin antimicrobial peptide (Hamp)	NM_032541	3.12
CD14 antigen (CD14)	NM_009841	−2.06
Immunoglobulin heavy chain C region (Igh-4)	M60430	−2.42
Lymphocyte antigen 6 complex, locus G6C (Ly6g6c)	NM_023463	−2.70
Adenosine deaminase (Ada)	NM_007398	−4.04
Defensin beta 4 (Defb4)	NM_019728	−4.48
Cell Cycle, Proliferation, and Transcription		
Epithelial cell transforming sequence 2 (Ect2)	NM_007900	6.22
Growth arrest-specific gene 1 (Gas1)	NM_008086	5.40
Zinc finger protein 318 (Zfp318)	NM_021346	3.58
Growth differentiation factor 10 (Gdf10)	L42114	2.82
Snail homolog 1 (Snai1)	NM_011427	−2.16
Heparin binding EGF-like growth factor (Hegfl)	NM_010415	−2.24
FBJ osteosarcoma oncogene (c-Fos)	AV026617	−2.32
Pituitary tumor-transforming 1 (Pttg1)	AV105428	−2.46
NFIL3E4BP4-like transcription factor (Nfil3)	AY061760	−2.50
v-Maf musculoaponeurotic fibrosarcoma (Maf)	NM_010755	−2.52
Methyl-CpG binding domain protein 1 (Mbd1)	AK007371	−2.56
Early growth response 2 (Egr2)	NM_009704	−3.12

Gene Name	**Genebank**	***Dmp1*$^{+/+}$ vs. *Dmp1*$^{-/-}$ (Lung)**
JunB	NM_008416	−3.20
Adrenomedullin (Adm)	NM_009627	−3.36
Amphiregulin (Areg)	NM_009704	−4.68
Early growth response 1 (Egr1)	NM_007913	−5.20
Metabolism and Enzymes		
Transmembrane protease, serine 3 (Tmprss3)	NM_080727	4.80
Metallothionein 1 (Mt1)	NM_013602	−2.32
Nocturnin	AF199491	−2.58
Metallothionein 2 (Mt2)	AA796766	−2.82
Cholesterol 25-hydroxylase (Ch25h)	NM_009890	−3.24
Calmodulin 4 (Calm4)	NM_020036	−3.52
Thrombospondin 1 (Tsp1)	M87276	−3.84
Metallothionein 4 (Mt4)	NM_008631	−5.29